



Magnetic Levitation Tribometer: A Point-Contact Friction

A. A. Vasko¹ · O. M. Braun¹ · O. A. Marchenko¹ · A. G. Naumovets¹

Received: 7 January 2018 / Accepted: 2 May 2018
© Springer Science+Business Media, LLC, part of Springer Nature 2018

Abstract

We developed a new magnetic levitation tribometer (MLT) to study point-contact friction via pendulum method. The device allows us to carry out fast and accurate point-contact measurement of friction between a pair of materials. The MTL parameters were found with the help of test experiments with the steel ball / glass plate pair. The friction coefficient values are coherent with the results known in the literature (Serway and Beichner in *Physics for scientists and engineers*, 5th edn, Saunders College Publishing, Orlando, 2000). The proposed MLT technique at loads lower than 10^{-3} N is very promising for non-destructive investigation of frictional properties of organic monolayers.

Keywords Point-contact friction measurements · Moment of inertia of pendulum · Kinetic friction coefficient

List of Symbols

ϕ	Angle deflection of pendulum
I_0	Pendulum moment of inertia
K_0	Impact of the external magnetic eld without extra mass
ω_0	Natural frequency without extra mass
Δm	Extra mass
l	Distance from the axis of pendulum to the center of extra mass
I	The total moment of inertia
K	Impact of the external magnetic field
ω	Natural frequency
γ	The damping coefficient
M	The total moment of force without friction
N	Applied normal load
μ_k	Velocity-dependent kinetic friction coefficient
μ_{k0}	Velocity-independent kinetic friction coefficient
r_0	Contact radius
Ω	Angular frequency
ψ	Dimensionless angle deflection of pendulum
ξ	Dimensionless damping coefficient
$\tilde{\omega}$	Dimensionless natural frequency
$\tilde{\gamma}$	Overall friction coefficient
M_f	The total moment of frictional force
τ	Dimensionless time

1 Introduction

As is known since the middle of the 20th century due to Bowder and Tabor [1], a frictional interface between two solid surfaces typically consists of many small contacts, usually of micrometer size [2]. Thus, these contacts play a key role in frictional properties of different systems. However, standard tribological experimental techniques, such as the classical inclined plane technique, measure only averaged properties, e.g., the total friction force, which is the sum of shear forces from all contacts [3]. For example, in the pin-on-disk experiments (e.g., see [4]), the contact size is of the order of millimeters or larger, i.e., it consists of many contacts.

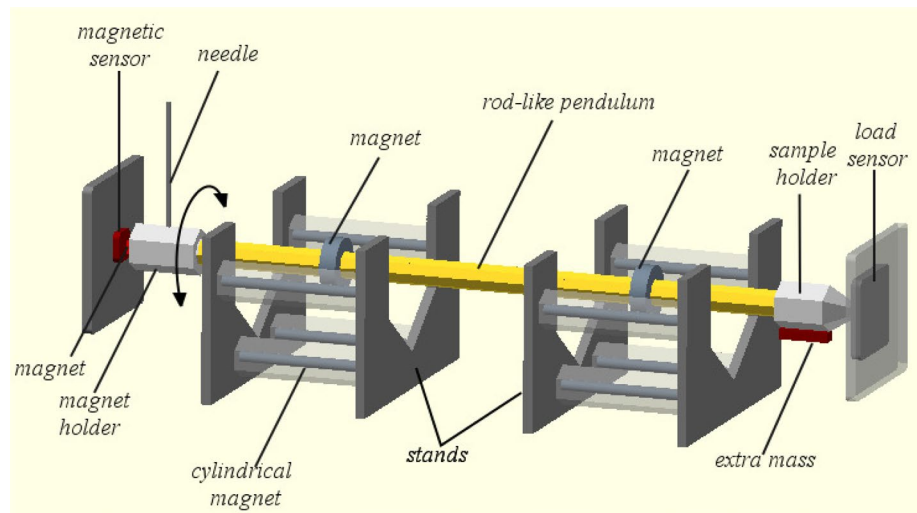
Besides, these experiments are often accompanied by wearing of surfaces [5]. On the other hand, recently developed tip-based techniques, such as the atomic force microscopy [6] (AFM) and friction force microscopy [7, 8] (FFM), operate with very small contacts, from atomic scale (single atoms) to nanometer size.

In the present paper, we describe a qualitatively new experimental method to measure friction in a single point-like contact. It uses a magnetic levitation tribometer (MLT)—a pendulum oscillating in an external magnetic field. Test measurements were carried out with a steel ball over the glass plate at different loads. This allowed us to find the parameters of the device such as the moment of inertia of pendulum I , the parameters of the magnetic field and the damping coefficient γ , and finally to extract the

✉ A. A. Vasko
artem.vasko@ukr.net

¹ Institute of Physics, National Academy of Sciences of Ukraine, 46 prospect Nauki, Kiev 03028, Ukraine

Fig. 1 The magnetic levitation tribometer. It consists of a rod-like pendulum, stands with magnets inside cylinders, the stand with magnetic sensor, and the stand with a sensor of normal load



friction coefficient μ . The proposed pendulum method can be sensitive enough to permit non-destructive regimes of measurements.

2 Experimental Set-Up

The experimental set-up, designed and built in order to investigate the coefficient of dry friction between two solid materials as well as the impact of a lubricant on friction between them, is shown in Fig. 1. The MLT consists of two basic elements, the rod-like pendulum and the stands with cylinders. A set of magnets inside cylinders and two magnets on pendulum allow it to keep a horizontal position. The fixing point at one side of the pendulum is a prerequisite for the system stability. Investigated materials are mounted at this point, one at the end of pendulum (steel ball) and the other on the vertical stand with a feedback system, the latter has a sensor to measure the normal load N which may be directly controlled by shifting the stands. One more magnet is placed on the opposite side of pendulum. With its help, every rotation of magnet is captured via a magnetic sensor. The initial position of the pendulum is controlled by stepper motor that smoothly deflects the pendulum from the equilibrium position and makes it to oscillate freely. The magnetic sensor continuously records the position of magnet until oscillations stop. The resulting data consist of the angle deflection of pendulum as a function of time $\phi(t)$.

To carry out test experiments, we used a spherical steel ball ($R = 0.8$ mm) and glass plate ($L \times W \times H = 20 \times 50 \times 2$ mm). Then, further experiments were performed with steel ball and Al, Cu, Ti, Ni, Mo plates ($L \times W \times H = 15 \times 15 \times 0.5$ mm). All experiments were done under controlled temperature and humidity.

3 Calibration of the Device

A typical experimental dependence is shown in Fig. 2. In order to calibrate our device, we made a series of experiments with a steel ball ($R = 0.8$ mm) on the glass surface. Neglecting by friction between the ball/glass pair and considering only small rotation angles so that $\sin \phi \approx \phi$, the motion equation for the angle $\phi(t)$ is

$$I\ddot{\phi} + \gamma I\dot{\phi} = M = -K\phi, \quad (1)$$

where I is the total moment of inertia, γ is the internal damping within MLT, M is the total moment of force, and K is an impact of the external magnetic field. The solution of this equation is trivial,

$$\phi(t) = \phi_0 \sin[\omega(t + t_0)] \exp(-\gamma t/2), \quad (2)$$

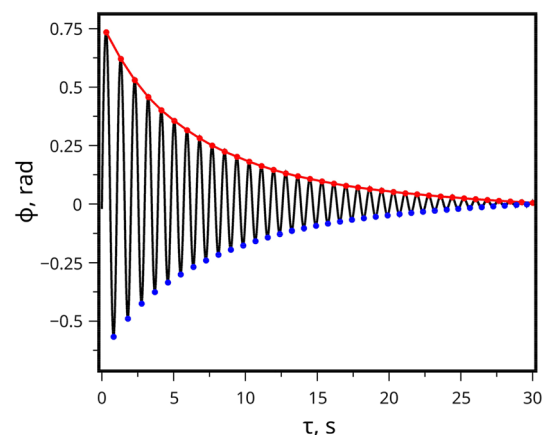


Fig. 2 The angle $\phi(t)$ for the load $N = 4.9 \times 10^{-2}$ N and extra mass $\Delta m = 3 \times 10^{-4}$ kg. Red/blue points indicate local maxima/minima, red solid curve shows the exponential decay with $\gamma = 0.266$ s $^{-1}$. (Color figure online)

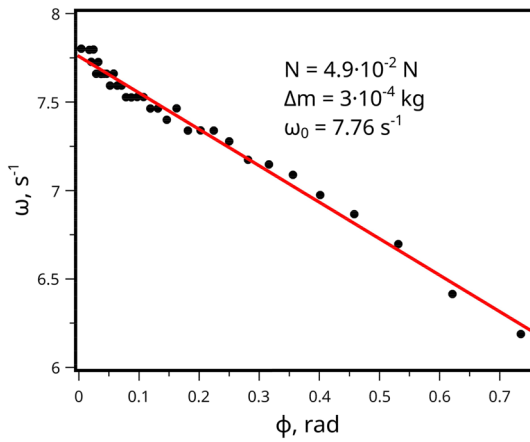


Fig. 3 The frequency versus amplitude. Black points correspond to experimental data, red curve is fitting with $\omega = 7.76 - 0.227\phi_n$

where $\omega^2 = K/I - \gamma^2/4$. The frequency ω may be found experimentally: Let us find all local maxima/minima ϕ_n of the dependence $\phi(t)$ (red/blue points in Fig. 2); then the interval between consequent maxima or minima gives the oscillation period T and thus the frequency $\omega = 2\pi/T$. Experimental data show that the frequency depends on the amplitude of oscillations ϕ_n (see Fig. 3).

The linear dependence $\omega(\phi_n)$ indicates that the potential well created by the magnetic field in the device, is in fact anharmonic, i.e., the potential energy is described by the expression $U(\phi) = \frac{1}{2}K\phi^2 - \varepsilon|\phi^3| + O(\phi^4)$ with some anharmonicity parameter ε . Therefore, we extracted the characteristic frequency, using the linear fit of the dependence $\omega(\phi_n)$ and taking the limit at zero amplitude, $\phi_n \rightarrow 0$, as demonstrated in Fig. 3.

In order to find the device parameters I and K , we used the following trick. We added an extra mass Δm on a distance l from the axis of pendulum to the center of extra mass ($l = 8$ mm, see Fig. 1). In this case $I = I_0 + l^2\Delta m$ and $K = K_0 + gl\Delta m$, where $g = 9.81$ m/s², so that

$$\omega^2(\Delta m) = \frac{K_0 + gl\Delta m}{I_0 + l^2\Delta m} - \frac{1}{4}\gamma^2. \tag{3}$$

Note that without damping ($\gamma = 0$) we have $\omega_0^2 \equiv \omega^2(0) = K_0/I_0$ and $\omega^2(\infty) = g/l$. Then, using three different masses $\Delta m = 0.3, 0.6,$ and 0.9 gram and fitting the dependence $\omega_0(\Delta m)$ with Eq. (3), we were able to find the parameters I_0 and K_0 (see an example in Fig. 4).

With this procedure we obtained the following results. The pendulum moment of inertia is $I_0 = 1.2 \times 10^{-6}$ kg m² (the same for all loads), while the parameters K_0 and ω_0 slightly depend on load (see Table 1).

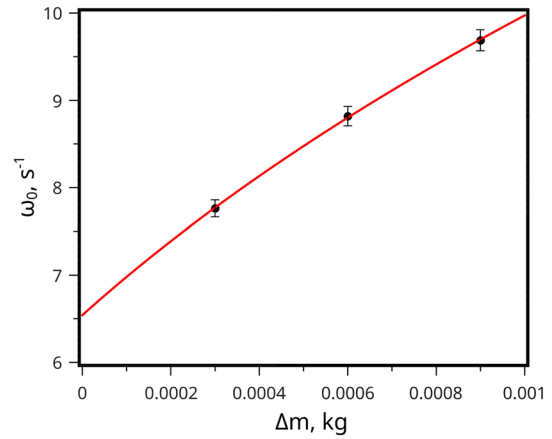


Fig. 4 The frequency ω_0 as a function of the extra mass Δm for the load $N = 4.9 \times 10^{-2}$ N

Table 1 Parameters of the device

Load (10^{-2} N)	K_0 (10^{-5} kg m ² s ⁻¹)	ω_0 (s ⁻¹)
3,92	5,27	6,67
4,9	5,44	6,54
5,89	5,76	6,35

4 Friction Coefficient

We used an optical method to determine the contact radius r_0 at different normal loads, and found that $r_0 = (1.85 \pm 0.1) \times 10^{-4}$ m for $N = 3.92 \times 10^{-2}$ N, $r_0 = (1.97 \pm 0.1) \times 10^{-4}$ m for $N = 4.9 \times 10^{-2}$ N, and $r_0 = (2.1 \pm 0.1) \times 10^{-4}$ m for $N = 5.89 \times 10^{-2}$ N.

Let us assume that the contact of steel ball and flat glass surface corresponds to the Hertz contact. In this case, the pressure distribution in the contact region is given by the expression

$$p(r) = p_0(1 - r^2/r_0^2)^{1/2}, \tag{4}$$

where p_0 is the maximal pressure in the center. Then, the normal load N for the contact is given by the expression

$$N = \int_0^{r_0} dr 2\pi r p(r). \tag{5}$$

Defining the velocity-dependent kinetic friction coefficient as¹

$$\mu_k(v) = \mu_{k0} + (I/N)\beta v, \tag{6}$$

¹ We included also a possible dependence of kinetic friction coefficient on sliding velocity, as proposed in [9], although for dry friction studied here it is usually negligible, $\beta = 0$.

where $v(r) = r\dot{\phi}$, the total moment of frictional force is given by

$$M_f = - \int_0^{r_0} [r\mu_k(v)p(r)] \cdot 2\pi r dr = M_{f0} + M_{fv}, \quad (7)$$

which after integration leads to the expressions

$$M_{f0} = -\frac{3\pi}{16} r_0 \mu_{k0} N \quad (8)$$

and

$$M_{fv} = -\frac{2}{5} I r_0^2 \beta \dot{\phi}. \quad (9)$$

Taking into account the glass/ball friction, the full motion equation may be written as

$$I\ddot{\phi} + \gamma I\dot{\phi} + K\phi = M_f, \quad (10)$$

which may be rewritten as

$$I\ddot{\phi} + \tilde{\gamma} I\dot{\phi} + K\phi = M_{f0} = -\mu_{k0} N_f \operatorname{sgn}(\dot{\phi}), \quad (11)$$

where $\tilde{\gamma} = \gamma + (2/5)r_0^2\beta$ and $N_f = (3\pi/16)r_0N$.

Dimensionless equation of motion can easily be rewritten as follows:

$$\ddot{\psi} + 2\xi\dot{\psi} + \psi = -\mu_{k0} \operatorname{sgn}(\dot{\psi}), \quad (12)$$

where $\psi = K\phi/N_f$, $2\xi = \tilde{\gamma}/\Omega$, $\Omega^2 = K/I$, and $\tau = \Omega t$. The exact solution of Eq. (12) may be found in Ref. [9]:

$$\psi + \mu_{k0} \operatorname{sgn}(\dot{\psi}) = [\psi_0 + \mu_{k0} \operatorname{sgn}(\dot{\psi})] e^{-\xi(\tau-\tau_0)} [\cos(\tilde{\omega}[\tau - \tau_0]) + \tilde{\beta} \sin(\tilde{\omega}[\tau - \tau_0])], \quad (13)$$

where $\tilde{\omega} = \sqrt{1 - \xi^2}$ and $\tilde{\beta} = \xi/\sqrt{1 - \xi^2}$. Exploring Eq. (13) for half-periods of oscillations from τ_n to $\tau_{n+1} = \tau_n + \pi/\tilde{\omega}$ and using the initial condition $\psi(0) = \psi_0$, $\dot{\psi}(0) = 0$, and also $\psi_n = \psi(\tau_n)$, we obtain an expression for μ_{k0} :

$$\mu_{k0} = \frac{\psi a^{2p} - \psi_{2p}}{1 + a^2 + 2 \sum_{i=1}^{2p-1} a^i}, \quad (14)$$

where $a = \exp(-\tilde{\beta}\pi)$.

5 Experimental Results

To extract the coefficient μ_{k0} , we discard the first 15 seconds of oscillation (see Fig. 5), where the anharmonicity of the potential well and a high dissipation of energy lead to a large error. In this way, we obtained a stable value of μ_{k0} (a plateau on the $\mu_{k0}(t)$ dependence, see Fig. 5) for a set of experimental regimes for the steel/glass pair (see Table 2).

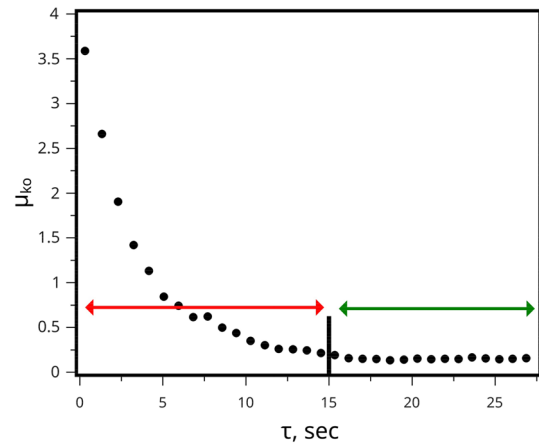


Fig. 5 Evolution of μ_{k0} versus time for the load $N = 4.9 \times 10^{-2}$ N and the extra mass $\Delta m = 3 \times 10^{-4}$ kg for the steel ball / glass pair. Stable region of oscillations indicated by green arrow corresponds to the kinetic friction coefficient $\mu_{k0} = 0.152$. (Color figure online)

Table 2 Kinetic friction coefficient μ_{k0} (the steel ball / glass pair)

Δm (10^{-4} kg)	Normal load N (10^{-2} N)		
	3.92	4.9	5.89
3	0.159 ± 0.005	0.152 ± 0.002	0.173 ± 0.003
6	0.153 ± 0.005	0.142 ± 0.005	0.148 ± 0.003
9	0.151 ± 0.003	0.151 ± 0.005	0.158 ± 0.005

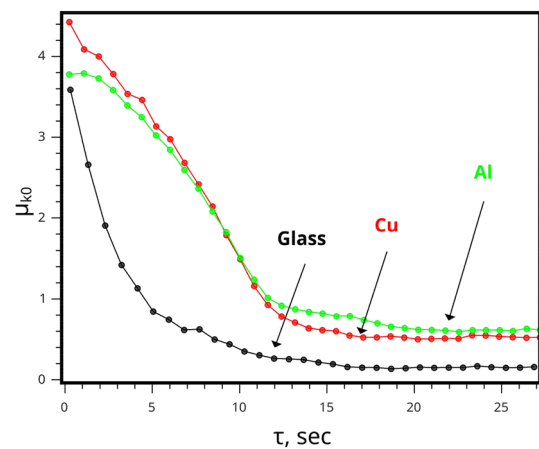


Fig. 6 Evolution of the coefficient $\mu_{k0}(\tau)$ for the steel ball over the Al, Cu and glass surfaces

Finally, we also measured the friction between the steel ball and different surfaces such as Al, Cu, Ni, Mo, and Au. The results are presented in Fig. 6 and Table 3. One can see a good agreement with known experimental data.

Table 3 Kinetic friction coefficient μ_{k0} for steel ball on different surfaces

Substrate	μ_{k0} within MLT	μ_{k0} in literature
Al	0.60 \div 0.61	0.61 [5]
Cu	0.50 \div 0.53	0.53 [5]
Glass	0.15 \div 0.17	–
Ni	0.59 \div 0.62	–
Mo	0.65 \div 0.66	–
Au	0.34 \div 0.35	–

6 Conclusions

Thus, we proposed the new approach for measuring friction using the magnetic levitation tribometer. The friction coefficient values are coherent with the results known in the literature [5]. Our device allows us to study friction with a single point-like contact of sub-millimeter size. We used the optical method to measure the contact area; for non-transparent substrates one may use the Hertz or JKR theory to estimate it. The MLT allows measurements for very low loads, which makes it suitable for non-destructive investigation of friction with monolayer organic lubricant films; we plan to proceed with corresponding experiments in a nearest future. The structure of surfaces and the lubricant film may easily be checked with STM/AFM technique before and after friction measurements. Moreover, in principle one may extract also a dependence of the kinetic friction coefficient on the sliding velocity in a single experimental run for a wide interval of

velocities. All these makes our technique very promising in looking for new lubricants, e.g., for nanodevices.

Acknowledgements The authors would like to thank A. Le Bot, J. Scheibert, and M. Sahli Riad for numerous helpful comments and discussions. This work was supported by CNRS-Ukraine PICS Grant No. 151539. O.B. was supported in part by COST Action MP1303.

References

1. Bowden, F.P., Tabor, D.: Friction and Lubrication of Solids. Clarendon, Oxford (1950)
2. Baumberger, T., Caroli, C.: Solid friction from stick-slip down to pinning and aging. *Adv. Phys.* **55**, 279–348 (2006)
3. Stachowiak, G.W., Batchelor, A.W., Stachowiak, G.B.: Experimental methods in tribology. *Tribol. Ser.* **44**, 1–354 (2004)
4. Belin, M., Kakizawa, M., Rigaud, E. and Martin, J.M.: Dual characterization of boundary friction thanks to the harmonic tribometer: identification of viscous and solid friction contributions. *J. Phys. Conf. Ser.* (2010). <https://doi.org/10.1088/1742-6596/258/1/012008>
5. Serway, R.A., Beichner, R.J.: Physics for Scientists and Engineers, 5th edn. Saunders College Publishing, Orlando, FL (2000)
6. Binnig, G., Quate, C.F., Gerber, C.: Atomic force microscope. *Phys. Rev. Lett.* (1986). <https://doi.org/10.1103/PhysRevLett.56.930>
7. Mate, C.M., McClelland, G.M., Erlandsson, R., Chang, S.: Atomic scale friction of a tungsten tip on a graphite surface. *Phys. Rev. Lett.* **59**, 1942–1945 (1987)
8. Mate, C.M.: Atomic scale friction. In: Bhushan, B. (ed.) *Handbook of Micro/Nano Tribology*. CRC Press, Boca Raton (1995)
9. Rigaud, E., Perret-Liaudet, J., Belin, M., Joly-Pottuz, L., Martin, J.-M.: An original dynamic tribotest to discriminate friction and viscous damping. *Tribol. Int.* **43**, 320–329 (2010)